Time-Lapse Full Waveform Inversion Application To Seismic Monitoring Of CO_2 Sequestration

Wubshet Alemie, Department of Physics, University of Alberta, alemie@ualberta.ca

Summary

Time-lapse seismic methods are among the geophysical techniques, which are being used for monitoring of subsurface changes by taking a series of observations over time. The time-lapse difference between baseline and monitored observations suffers with artifacts, which sometimes may have equivalent strength that of the true signal of interest. Therefore, developing seismic data processing and inversion methods, which are suitable specific to time lapse data, is crucial. To address this issue in the inversion framework, independent and joint time-lapse full waveform inversion strategies with a 2D Total Variation (TV) regularization along with Limited-memory Broyden-Fletcher-Goldfarb-Shanno (L-BFGS) algorithm are presented with synthetic examples, which mimics monitoring of CO_2 in Geo-sequestration. The preliminary results of the inversion show slight advantage of joint inversion in attenuating small fluctuations in the time-lapse velocity difference as compared to the independent inversion.

Introduction

Seismic inversion is the most widely used subsurface imaging technique. This technique provides high-resolution complex geological information from seismic data to characterize the subsurface qualitatively and quantitatively. Migration and FWI, in particular, are advanced techniques for high-resolution subsurface imaging (Pratt, 1999; Hu et al., 2009; Brossier, 2011; Ma and Hale, 2012). However, those traditional available imaging algorithms are not effective enough to address issues associated with time-lapse data; mainly for monitoring of fluid dynamics such as water, oil and gas trapped with in rock matrix. The application of FWI, in particular, specific to time-lapse data inversion are not well explored. There are very few attempts in developing time-lapse seismic inversion for the purpose of monitoring. For instance, linearized time-lapse inversion by Ayeni and Biondi (2011); this particular work addressed the problem by incorporating regularization techniques in the inversion algorithm to jointly invert successive time-frames. However, the non-linearity of the geophysical problem was not addressed. Queibetaer and Singh (2010) suggested full waveform inversion over migration for better indication of CO_2 signature in CO_2 sequestration monitoring. Our goal is to extend the FWI algorithm into a joint time-lapse inversion algorithm with 2D TV-Regularization, which is capable of attenuating artifacts introduced due to the time-lapse nature of the problem. This formulation is similar to double difference time-lapse full waveform inversion (Lin et al., 2012) but with different parametrization. Note that TV-Regularization has an effect of edge preserving denoising and has been used with success in seismic imaging (Lin et al., 2012; Anagaw and Sacchi, 2011).

To this end, the seismic data is modelled with 2D frequency domain acoustic wave equation with PML boundary conditions and discretized with second order in space finite difference. The resulting linear equation is highly sparse and solved by sparse MUMPS solver. The inversion algorithm is derived via adjoint state method and uses L-BFGS algorithm for calculating search direction and Wolf conditions to choose step lengths to update solution at each iteration. Two inversion strategies are explored. The first one is Independent inversion; doing independent inversion for each time-frame. The second case is a joint inversion of the baseline and monitored frames, which are inter linked by the TV-Regularization. The time-lapse velocity difference is obtained by taking the difference between baseline and monitored inversion results. These algorithms are demonstrated by synthetic examples; a velocity model which mimics saline aquifer CO_2 sequestration model. A time-lapse velocity model is generated taking into account reservoir conditions and using Biot-Gassmann fluid substitution technique.

Theory

Forward Modelling

The seismic data is modelled by constant density acoustic wave equation in frequency domain with second order in space finite difference discretization,

$$\left[\frac{\partial}{\partial x}\left(\frac{\partial}{\partial x}\right)+\frac{\partial}{\partial z}\left(\frac{\partial}{\partial z}\right)+(\omega/c)^2)\right]U(\mathbf{X})=S(\mathbf{X})\delta(\mathbf{X_s}-\mathbf{X}), \tag{1}$$

where ω is the angular frequency, U is the wavefield in 2D space at the given frequency, S is the excitation source at position $X_s = X(x_s, z_s)$. Absorbing Boundary Condition (ABC) and Perfectly Matching Layers (PML) techniques are widely used boundary conditions in many research areas (Engquist and Majda, 1977; Berenger, 1994). The PML is incorporated into the acoustic wave equation by transforming the wave equation into stretched coordinate system (Berenger, 1994). Thus, discretizing the wave equation with finite difference leads to the following matrix equation,

$$\mathbf{AU}=\mathbf{S}, \tag{2}$$

where $\mathbf{A}$ is a highly sparse matrix operator which takes into account the finite difference coefficients, the frequency and the medium property. The wave field, $\mathbf{U}$, and the source, $\mathbf{S}$, have the same size in 2D space reshaped into column vectors. The source vector has non-zero value at the source location and zero elsewhere. The solution of wave equation results a monochromatic wave field i.e wave field in space at a single frequency. The frequency domain data at receiver location can be obtained by, $\mathbf{RU}=\mathbf{d}^{cal}$, where $\mathbf{R}$ is an operator which represents the receiver array i.e it is a an operator which picks a data value of the 2D wave field at the receiver positions.

Independent Inversion

The inversion algorithm is derived in least squares sense by defining a cost function, which is a function of data residual (the difference between observed data and calculated data) and additional regularization term (prior information). In traditional time-lapse full waveform inversion is, simply, applying independent inversion for each time-frames (t_i) and taking differences to get the time-lapse signatures. Under the assumption that the data residual represents Gaussian noise, the regularized cost function for each time-frame t_i can be written as,

$$J_{t_i}(\mathbf{m}_{t_i})=\frac{1}{2}\sum_{i_{\omega_g}}^{N_{\omega_g}}\sum_{i_s}^{N_s}\triangle\mathbf{d}(\mathbf{m}_{t_i})^{\dagger}\triangle\mathbf{d}(\mathbf{m}_{t_i})+\mu R_i(\mathbf{m}_{t_i}-\mathbf{m}_I), \tag{3}$$

where $\triangle\mathbf{d}(\mathbf{m})=\mathbf{d}^{obs}-\mathbf{d}^{cal}$, the observed data $\mathbf{d}^{obs}$ and the calculated data $\mathbf{d}^{cal}$. The goal is find a 2D velocity model or earth medium property that minimizes the objective function by honouring the input data. The expression for the regularization R_i depends on choice of prior information. The 2D total variation regularization given by Equation 4 is chosen to be the regularization function. It is the most widely used method in many fields of study for image edge-preserving denoising. In our particular problem, the directional first order undivided difference operators are applied on the difference between the models of interest ($\mathbf{m}_{t_i}$) and their corresponding reference models ($\mathbf{m}_{r_i}$). Thus, the expression of the regularization has a form

$$R_i(\mathbf{m}_{t_i}-\mathbf{m}_I)=\sum_{l=1}^{L}\sqrt{\left([\mathbf{D}_x(\mathbf{m}_{t_i}-\mathbf{m}_I)]_l^2+[\mathbf{D}_z(\mathbf{m}_{t_i}-\mathbf{m}_I)]_l^2+\beta^2\right)} \tag{4}$$

where $\mathbf{D}_x$ and $\mathbf{D}_z$ are the lateral and depth direction first order undivided difference operators, β is a parameter that allows differentiability at zero. This regularization helps to filter out outliers and also very small fluctuations in the image which can be considered as noise. For independent time-lapse inversion, we use the initial velocity model ($\mathbf{m}_I$) as reference model for all time frames.

Gradient

The first order derivative of the cost function given by Equation 3 with respect to the model parameter, $m_{t_i}^j$, and generalized into all model parameters $j = 1,2,3,4,..,N$, at a given time-frame can be easily found,

$$\nabla_{\mathbf{m}_{t_i}} J_{t_i}(\mathbf{m}_{t_i}) = \sum_{i_{\omega_g}}^{N_{\omega_g}} \sum_{i_s}^{N_s} \Re\{\mathbf{f}^T [\mathbf{A}^{-1}]^T \triangle \mathbf{d}(\mathbf{m}_{t_i})^*\}_{t_i} + \mu_{t_i}(\Omega_{t_i}^x + \Omega_{t_i}^z) \ , \tag{5}$$

where each column of the diagonal matrix $\mathbf{f}$ is a virtual source given by $\mathbf{f}^j = \left[\frac{\partial \mathbf{A}}{\partial m_{t_i}^j}\right]\mathbf{U}_s$, and the expressions in the second term are

$$\Omega_{t_i}^x = \mathbf{D}_x^T \mathbf{Q}_{t_i}^{x,z} \mathbf{D}_x(\mathbf{m}_{t_i} - \mathbf{m}_I), \Omega_{t_i}^z = \mathbf{D}_z^T \mathbf{Q}_{t_i}^{x,z} \mathbf{D}_z(\mathbf{m}_{t_i} - \mathbf{m}_I), \tag{6}$$

where

$$\left[\mathbf{Q}_{t_i}^{x,z}\right]_{ll} = \frac{1}{\sqrt{\left([\mathbf{D}_x(\mathbf{m}_{t_i} - \mathbf{m}_I)]_l^2 + [\mathbf{D}_z(\mathbf{m}_{t_i} - \mathbf{m}_I)]_l^2 + \beta^2\right.}}. \tag{7}$$

The matrix $\mathbf{Q}_{t_i}^x$ and $\mathbf{Q}_{t_i}^z$ are diagonal matrices. The calculated source wave field is denoted by $\mathbf{U}_s$. Note that the actions of the first order undivided difference operators are implemented in the algorithm with matrix free operators.

The model parameter m is parametrized such that $m = \frac{1}{c}$. The model parameter can also parametrized in various ways (Pratt et al., 1998). For the time-lapse inversion, we avoid the direct calculation of the Hessian using L-BFGS algorithm. The output of the L-BFGS algorithm is a search direction by building the inverse of Hessian implicitly from a certain number of most recent gradient information. The search direction is denoted by $\triangle \mathbf{p}$. The solution is updated with the expression,

$$\mathbf{m}^{k+1} = \mathbf{m}^k + \gamma \triangle \mathbf{p}. \tag{8}$$

A parameter γ is introduced as scale factor. This is a step length which should be determined such that the solution is updated into the decent direction. Inexact line search algorithms can be used in order to get acceptable step lengths.

Joint Inversion

The objective function of the regularized joint time-lapse full waveform inversion is defined as sum of the individual objective functions of each time-frame which depends on the data residuals and the corresponding model regularizations. For N_f frames, the objective function with regularization can be written as

$$J(\mathbf{m}) = \sum_{i=0}^{N_f - 1} J_d^{t_i}(\mathbf{m}_{t_i}) + \mu_0 R_0 + \mu_1 R_1 +, \cdots, + \mu_{N_f - 1} R_{N_f - 1}, \tag{9}$$

where $R_0(\mathbf{m}_{t_0} - \mathbf{m}_{r_0}), R_1(\mathbf{m}_{t_1} - \mathbf{m}_{r_1}), R_2(\mathbf{m}_{t_2} - \mathbf{m}_{r_2}), ...$ are regularization terms. The model regularizations inter-link the base-line model parameter with models of successive time frames via the 2D TV-Regularization. The regularization, R_i, depends on the difference between the model $\mathbf{m}_{t_i}$ and a corresponding reference model $\mathbf{m}_{r_i}$. At a given iteration (k), the baseline time-frame uses the starting velocity model as reference model, and the other successive time-frames use the inversion result of the baseline time-frame obtained at the previous iteration $(k-1)$. This objective function is defied in more general form with more than two time-frames. For demonstrating the joint time-lapse inversion, we take only two time-frames for simplicity. For two time-frames (t_0 and t_1), the gradient becomes,

$$\nabla_{\mathbf{m}} J(\mathbf{m}_0) = \begin{bmatrix} \sum_{i_{\omega_g}}^{N_{\omega_g}} \sum_{i_s}^{N_s} \Re\{\mathbf{f}^T [\mathbf{A}^{-1}]^T \triangle \mathbf{d}(\mathbf{m}_{t_0})^*\}_{t_0} + \mu_{t_0}(\Omega_{t_0}^x + \Omega_0^z) \\ \sum_{i_{\omega_g}}^{N_{\omega_g}} \sum_{i_s}^{N_s} \Re\{\mathbf{f}^T [\mathbf{A}^{-1}]^T \triangle \mathbf{d}(\mathbf{m}_{t_0})^*\}_{t_1} + \mu_{t_1}(\blacksquare_{t_1}^x + \blacksquare_{t_1}^z) \end{bmatrix}, \tag{10}$$

where

$$\Omega_{t_i}^x \quad = \quad \mathbf{D}_x^T \mathbf{Q}_{t_i}^x \mathbf{D}_x(\mathbf{m}_{t_i} - \mathbf{m}_{r_i}), \Omega_{t_i}^z = \mathbf{D}_z^T \mathbf{Q}_{t_i}^z \mathbf{D}_z(\mathbf{m}_{t_i} - \mathbf{m}_{r_i}) \tag{11}$$

and $\left[\mathbf{Q}_{t_i}^{x,z}\right]_{ll} = \frac{1}{\sqrt{\left([\mathbf{D}_x(\mathbf{m}_{t_i}-\mathbf{m}_{r_i})]_l^2+[\mathbf{D}_z(\mathbf{m}_{t_i}-\mathbf{m}_{r_i})]_l^2+\beta^2\right.}}$. In the next section, synthetic examples are given with a velocity model that mimics Sleipner Field CO_2 sequestration.

Synthetic Examples

Sleipner Field Saline Aquifier CO_2 Storage (SACS) in Norway is one of the few projects where CO_2 geo-sequestration has become practical to mitigate green house gas emission(Chadwick et al., 2008). Various monitoring techniques including the seismic methods are being used to monitor the injected CO_2 into Utsira sand saline aquifer reservoir. The reservoir is located from 800 to 1000 m deep and has thickness of between 200 m and 300 m (Zweigel et al., 2001). Since this project is very well explored and documented, we chose to use the available information in the literature to generate velocity model making use of the Biot-Gassmann's fluid substitution steps which help to estimate physical parameters. The Biot-Gassmann's equation (Gassmann, 1951; Biot, 1956) along with Batzle-Wang equations (Batzle and Wang, 1992) are used to estimate unknown fluid parameters from known reservoir conditions. The the P-wave velocity generated by the fluid substitution model at different saturation level is used to build the 2D velocity model for a constant density acoustic wave equation modelling presented in Equation 1 to mimic the time lapse change. This model has a shale seal above the Utsira sand reservoir. The true baseline 2D velocity model is shown in Figure 1(a). The true velocity model which represents time-lapse velocity after CO_2 injection is shown in 1(b). Each of the models has *2.796 km* in lateral direction and *1.196 km* deep with a square gird size of *4 m* by *4 m*. The true time-lapse change in velocity is also shown in Figure 2(a). The true velocity models and a Ricker wavelet with central frequency *30 Hz* for source excitation are used to generate synthetic data; a total of *70* shots each separated by *40 m* with *348* receivers each separated by *8 m*.

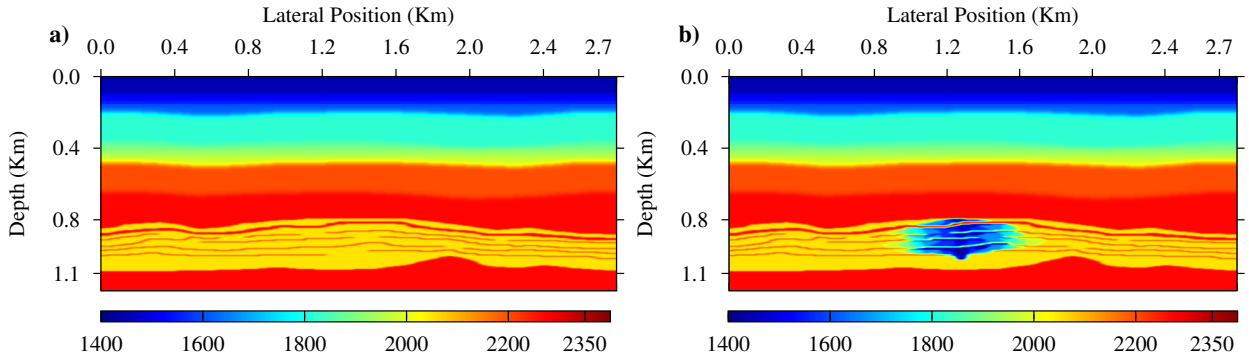

Figure 1 *CO_2 sequestration model (a) true base-line velocity model and (b) true velocity model after injection.*

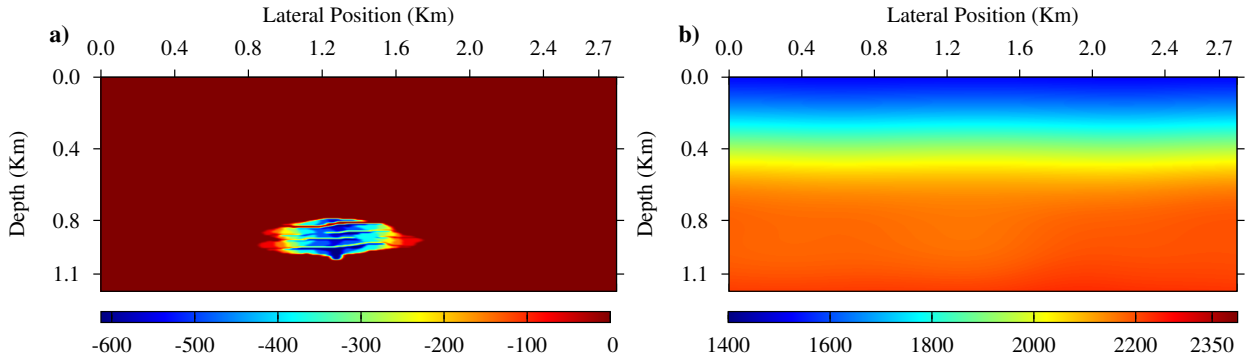

Figure 2 *CO_2 sequestration model (a) true time-lapse velocity difference and (b) starting velocity model for inversion.*

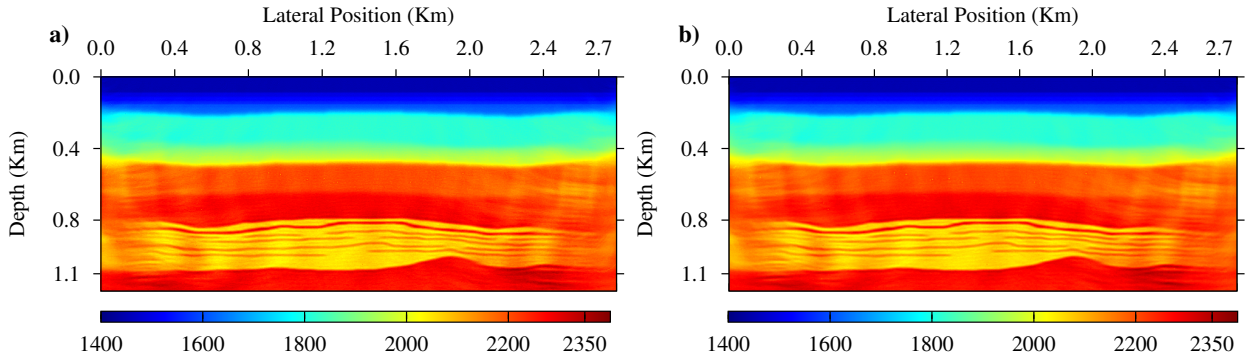

Figure 3 *The CO_2 sequestration model base-line inversion results (a) by independent inversion and (b) by joint inversion algorithms.*

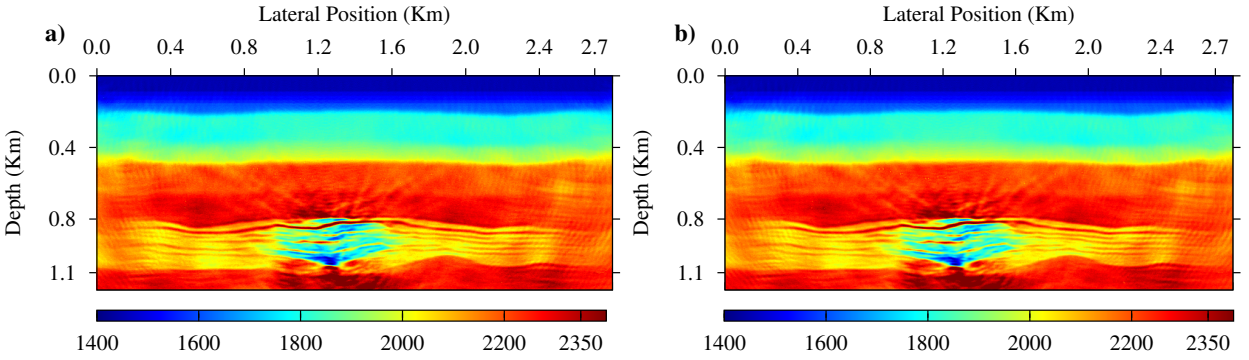

Figure 4 *The CO_2 sequestration model monitored inversion results (a) by independent inversion and (b) by joint inversion algorithms.*

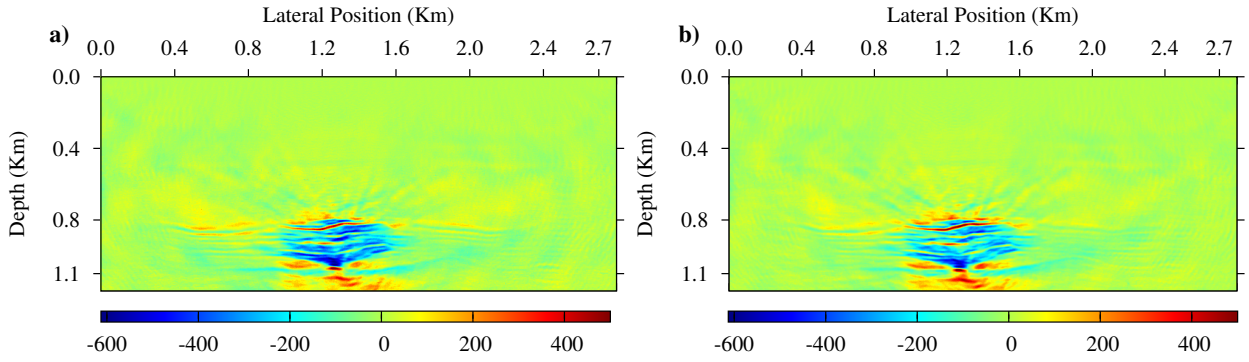

Figure 5 *The CO_2 sequestration model time-lapse differences (a) by independent inversion and (b) by joint inversion algorithms.*

In this synthetic inversion example, a smooth starting velocity model shown in Figure 2(b), nearly a linearly increasing velocity model, is used. The inversion was run for five selected group frequencies; each of them have three frequencies. The entire frequency ranges from 3.66 Hz to 68.4 Hz. The algorithm runs a maximum iteration of *60* for each group frequencies. Figure 3(a) and 3(b) are baseline inversion results by independent and joint inversion algorithms respectively. Figures 4(a) and 4(b) are monitored inversion results by independent and joint inversion algorithms, respectively. Figures 5(a) and 5(b) are time-lapse difference results by independent and joint inversion algorithms respectively.

CONCLUSIONS

The preliminary results of the inversion in the given examples show slight advantage of joint inversion in attenuating artifacts in the time-lapse velocity difference. Relatively strong changes just below the reservoirs could be the effect of velocity pushdown or due to the large deviation of the starting velocity model from the true velocity model or both. It worth mentioning that the same starting velocity model was used for both baseline and monitored inversions. The TV-regularization is sensitive to the choice of the parameter β. Large values destroys edge-preserving denoising ability. On the other hand, very small values of β sometime lead to instability in the inversion. With the proper choice of β, the regularization parameter μ controls the weight given to the regularization term. Therefore, well balanced choice of these parameters is crucial. The performance of the inversion algorithms need to be explored against various noise levels. In addition, it is important to assess the algorithm against the absence of low frequency data, different starting velocity models, and computation time cost.

ACKNOWLEDGMENTS

We wish to thank Carbon Management Canada (CMC-NCE) and Signal Analysis And Imaging Group in supporting this research.

References

Anagaw, A. Y. and M. D. Sacchi. "Full Waveform Inversion with Total Variation Regularization." *Recovery - CSPG CSEG CWLS Convention* (2011).

Ayeni, Gboyega and Biondo Biondi. "Wave-equation inversion of time-lapse seismic data sets." *SEG Technical Program Expanded Abstracts* 30 (2011): 4149–4154.

Batzle, M. and Z. Wang. "Seismic properties of pore fluids." *Geophysics* 57 (1992): 1396–1408.

Berenger, J. P. "A perfectly matched layer for the absorption of electromagnetic waves." *J. Computational Physics* 114 (1994): 185–200.

Biot, M.A. "Theory of propagation of elastic waves in fluid-saturated porous solid Part I: low frequency range." *Journal of the Acoustical Society of America* 28 (1956): 168–178.

Brossier, R. "Two-dimensional frequency-domain visco-elastic full waveform inversion: Parallel algorithms, optimization and performance." *Computers and Geosciences* 37 (2011): 444 – 455.

Chadwick, R.A, R. Arts, C. Bernstone, F. May, S. Thibeau, and P. Zweigel. "Best Practice For The Storage of CO2 In Saline Aquifers." *British Geological Survey Occasional Publication* (2008).

Engquist, B. and A. Majda. "Absorbing boundary conditions for the numerical simulation of waves. Mathematical Computation." *Mathematical Computation* 31 (1977): 629–651.

Gassmann, F. "Elastic Waves Through a Packing of Spheres." *Geophysics* 16 (October 1951): 673.

Hu, W., A. Abubakar, and T. M. Habashy. "Simultaneous multifrequency inversion of full-waveform seismic data." *Geophysics* 74 (2009): R1–14.

Lin, Y., L. Huang, and Z. Zhang. "Quantifying geophysical properties in small regions with in Enhanced Geothermal Systems (EGS)." *Thirty-Seven Workshop on Geothermal Reservoir Engineering, Stanford University, Stanford, California* (2012).

Ma, Yong and Dave Hale. "Quasi-Newton full-waveform inversion with a projected Hessian matrix." *Geophysics* 77 (2012): R207 – R2016.

Pratt, R. G. "Seismic waveform inversion in the frequency domain. Part I: Theory and verification in a physical scale model." *Geophysics* 64 (1999): 888–901.

Pratt, R. G, C .S. Shin, and G. J. Hicks. "GaussÐNewton and full Newton methods in frequency-space seismic waveform inversion." *Geophysics J. Int* 133 (1998): 341–362.

Queibetaer, M. and S. Singh. "Time lapse seismic monitoring of CO_2 sequestration at Sleipner using time domain 2D full waveform inversion." *SEG Technical Program Expanded Abstracts* 29 (2010): 2875–2879.

Zweigel, P., R. Arts, T. Bidstrup, R.A. Chadwick, O. Eiken, U. Gregersen, M. Hamborg, P. Johansessen, G.A. Kirby, L. Kristensen, and E. Lindeberg. "Results and Experiences from the first industrial-scale underground CO2 sequestration case, at Sleipner Field, Central North Sea." *American Association of Petroleum Geologists, Annual Meeting, Denver* 6 (2001).